



# Evaluation of the input site and characteristics of the antegrade fast pathway based on three-dimensional bi-atrial stimulus-ventricle mapping

Kazuhiisa Matsumoto<sup>1</sup> · Takeshi Tobiume<sup>1</sup> · Tomomi Matsuura<sup>1</sup> · Takayuki Ise<sup>1</sup> · Kenya Kusunose<sup>1</sup> · Koji Yamaguchi<sup>1</sup> · Shusuke Yagi<sup>1</sup> · Daijyu Fukuda<sup>1</sup> · Tetsuzo Wakatsuki<sup>1</sup> · Hirotsugu Yamada<sup>1</sup> · Takeshi Soeki<sup>1</sup> · Masataka Sata<sup>1</sup>

Received: 31 March 2021 / Accepted: 22 June 2021  
© The Author(s) 2021

## Abstract

**Purpose** Previous studies examined the right atrial (RA) input site of the antegrade fast pathway (AFp) (AFpI). However, the left atrial (LA) input to the atrioventricular (AV) node has not been extensively evaluated. In this study, we created three-dimensional (3-D) bi-atrial stimulus-ventricle (St-V) maps and analyzed the input site and characteristics of the AFp in both the RA and LA.

**Methods** Forty-four patients diagnosed with atrial fibrillation or WPW syndrome were included in this study. Three-dimensional bi-atrial St-V mapping was performed using an electroanatomical mapping system. Sites exhibiting the minimal St-V interval (MinSt-V) were defined as AFpIs and were classified into seven segments, four in the RA (F, S, M, and I) and three in the LA (M1, M2, and M3). By combining the MinSt-V in the RA and LA, the AFpIs were classified into three types: RA, LA, and bi-atrial (BA) types. The clinical and electrophysiological characteristics were compared.

**Results** AFpIs were most frequently observed at site S in the RA (34%) and M2 in the LA (50%), and the BA type was the most common (57%). AFpIs in the LA were recognized in 75% of the patients. There were no clinical or electrophysiological indicators for predicting AFpI sites.

**Conclusions** Three-dimensional bi-atrial St-V maps could classify AFpIs in both the RA and LA. AFpIs in the LA were frequently recognized. There were no significant clinical or electrophysiological indicators for predicting AFpI sites, and 3-D bi-atrial St-V mapping was the only method to reveal the precise AFp input site.

**Keywords** Antegrade fast pathway · St-V map · St-H map · Left atrial input · Right atrial input

## Abbreviations

|          |                              |               |   |    |
|----------|------------------------------|---------------|---|----|
| RA       | Right atrium/right atrial    | IDF           | Inferiorly dislocated AFp   |    |
| LA       | Left atrium/left atrial      | Pi            | Pacing site   | 37 |
| BA       | Bi-atrial                    | TOK           | Triangle of Koch  | 38 |
| A-H      | Atrial-His                   | MA            | Mitral annulus  | 39 |
| H-V      | His-ventricle                | TA            | Tricuspid annulus   | 40 |
| AFp      | Antegrade fast pathway       | St-H interval | Interval between the stimulation artifact and His bundle electrogram                            | 41 |
| AFpI     | Input site of AFp to the AVN | St-V interval | Interval between the stimulation artifact and peak of the QRS wave in lead                      | 42 |
| AFpI(RA) | AFpI in the RA               | MinSt-V       | The site showing the minimal St-V interval  | 44 |
| AFpI(LA) | AFpI in the LA               | MinSt-V(RA)   | MinSt-V in RA   | 45 |
|          |                              | MinSt-V(LA)   | MinSt-V in LA   | 46 |
|          |                              | VAT           | Ventricular activation time (the time from the onset of the QRS wave to the peak of the R wave) | 47 |

✉ Kazuhiisa Matsumoto  
matsumoto.kazuhiisa@tokushima-u.ac.jp

**AGI**<sup>1</sup> Department of Cardiology, Tokushima University Hospital, 3-18-15 Kuramoto-cho, Tokushima City, Tokushima 770-8501, Japan

## 1 Introduction

The exit site of the retrograde fast pathway (RFp) from the atrioventricular node (AVN) can be determined by mapping the earliest activation site in the atrium during constant pacing from the ventricle. On the other hand, the input site of the antegrade fast pathway (AFp) to the AVN has been very difficult to determine and only stimulus-His (St-H) mapping can identify the input site of the AFp to the AVN (AFpI) [1–5]. The use of a three-dimensional (3-D) mapping system makes identification of the exact location of the AFpI easier to determine [4, 5]. Previous studies, however, have examined the AFpI only in the right atrium (RA) (AFpI[RA]). The left atrial (LA) input to the AVN has not been extensively evaluated and only Gonzalez et al. have suggested that an AFpI exists in the LA (AFpI[LA]) with high probability in 95% of patients [6]. In this study, we created 3-D bi-atrial stimulus-ventricle (St-V) maps, which were equivalent to St-H maps, and analyzed the input site and characteristics of the AFp in both the RA and LA.

## 2 Methods

### 2.1 Study population

From June 1, 2019, to August 31, 2020, forty-four consecutive patients (31 men and 13 women,  $64 \pm 14$  years, range 25 to 80 years) with atrial fibrillation (AF) (18 paroxysmal and 16 persistent) or Wolff-Parkinson-White (WPW) syndrome with a left free wall accessory pathway who underwent catheter ablation were included in this study. Patients with first degree atrioventricular block and left bundle branch block were excluded because an AFp might not exist in the former and because transient AV block during mapping might occur in the latter. The institutional review board of Tokushima University approved the study protocol. Written informed consent was obtained from all patients.

### 2.2 Electrophysiological study

Patients with atrial fibrillation were studied under deep sedation with a continuous infusion of propofol. They were on a ventilator and underwent continuous monitoring of the blood pressure, oxygen saturation, and bispectral index. Patients with WPW syndrome were studied under local anesthesia using xylocaine. Venous access was established percutaneously from the right jugular vein and right femoral vein to introduce electrode catheters into the RA, right ventricle (RV), coronary sinus (CS), and LA. A His bundle electrogram recording catheter (His) was used in the case of WPW syndrome, but not in the case of AF. All patients required

a transseptal left heart catheterization for a pulmonary vein isolation or accessory pathway ablation. To record the electrocardiogram from the RA and CS, a 6-Fr catheter with 20 electrodes (BeeAT; Japan Lifeline, Tokyo) was inserted via the right jugular vein into the CS. A 5-Fr catheter with 5 electrodes (Arma, Century Medical Inc., Tokyo, Japan) was positioned in the RV apex (RVA). The CARTO®3 System (Biosense Webster, Irvine, California) was used for 3-D mapping in all patients. The bipolar electrocardiograms were filtered at 30–400 Hz for the electrophysiological analysis (CardioLab, GE Healthcare Japan, Tokyo).

### 2.3 Identifying the input site of the antegrade fast pathway using 3-D bi-atrial St-V maps

During the waiting period after the ablation, 3-D bi-atrial St-V maps for identifying the AFpI were created in all patients during constant atrial pacing at 100 ppm (600 ms) from a 7-Fr irrigation catheter (Thermocool SmartTouch SF, Biosense Webster). The pacing output was set at 3–4 V/1 ms in order to avoid capturing the AVN, His bundle, and ventricles. As shown in Fig. 1, constant pacing was performed at one pacing site (Pi) and, after reaching a steady state, the interval between the stimulation artifact and peak of the QRS wave in lead II (St-V interval) was measured. Data regarding both the location of the pacing site (Pi) and St-V interval at the Pi were stored on the 3-D map. Then, the pacing catheter was moved to the next site (Pi + 1). The AFpI was defined as the site exhibiting the minimal St-V interval (MinSt-V). The AFpI[RA] and AFpI[LA] were defined as the MinSt-V in the RA (MinSt-V[RA]) and LA (MinSt-V[LA]), respectively. The sites where the His bundle electrocardiogram was recorded were also stored on the 3-D map during sinus rhythm to identify the apex of the triangle of Koch (TOK) without the electrocardiographic information, and the A-H interval during sinus rhythm was measured at those sites. The anatomical information related to the roof and floor of the CS ostium, tricuspid annulus, and mitral annulus were also stored on the 3-D map.

### 2.4 Classification of the input site of the antegrade fast pathway

As shown in Fig. 2, for the classification of the AFpI, the atrial septum was subdivided into seven segments, four on the RA aspect and three on the LA side. In the RA, the TOK was classified into three equidistant parts: superior, middle, and inferior thirds defined as sites S, M, and I, respectively. Also, the part posterior to the TOK was defined as site F. If the AFpI was located at site M or I, the AFpI was defined as an inferiorly dislocated AFp (IDF). In the LA, the AFpI was classified into three segments along the mitral annulus (MA): the 6–7 o'clock, 7–8 o'clock, and 8–9 o'clock directions along the mitral annulus were labeled as sites M1, M2, and M3, respectively.

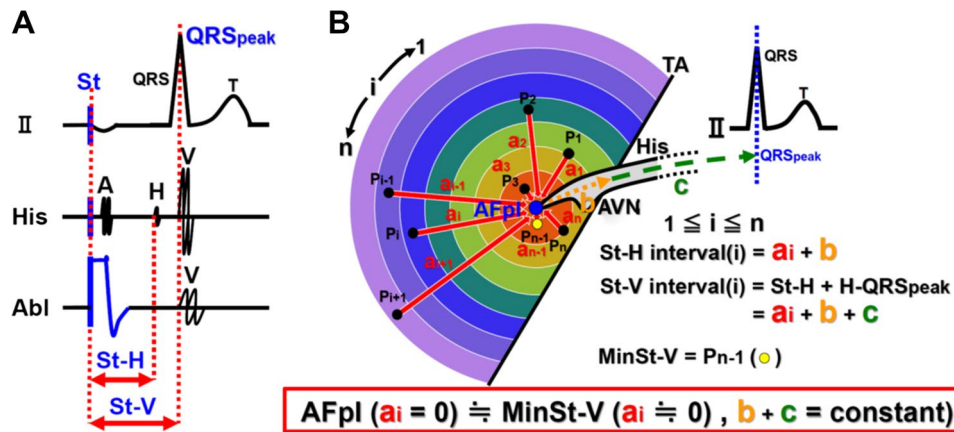


**Fig. 1** Schematic presentation of the method of St-V mapping (intra-cardiac electrogram (A) and electroanatomical map (B)). (A) a: During constant pacing from Abl catheter, St-V interval, which means the conduction time between the stimulation artifact and the peak of QRS wave in lead II, was measured at each pacing site. Pacing output was set at 3–4 V/1 ms (B) St-V interval of the *i*th pacing site was shown as “ $a_i + b + c$ .” At MinSt-V,  $a_i$  was approximately zero and MinSt-V was almost identical with AFpI, where  $a_i$  was equal to zero. His, His bundle catheter; Abl, ablation catheter; St, stimulus; A, atrial electro-

gram; H, His bundle electrogram; V, ventricular electrogram; St-H, stimulus-His; St-V, stimulus-ventricle; AVN, atrioventricular node; AFp, antegrade fast pathway; AFpI, input site of AFp to AVN;  $P_i$ , *i*th pacing site;  $P_n$ , *n*th pacing site; St-H interval(*i*), St-H interval of the *i*th pacing site; St-V interval(*i*), St-V interval of the *i*th pacing site; MinSt-V, the pacing site showing the minimal St-V interval;  $a_i$ , conduction time between the pacing site and AFpI;  $b$ , conduction time between AFpI and His bundle electrogram;  $c$ , conduction time between His bundle electrogram and the peak of QRS wave in lead II

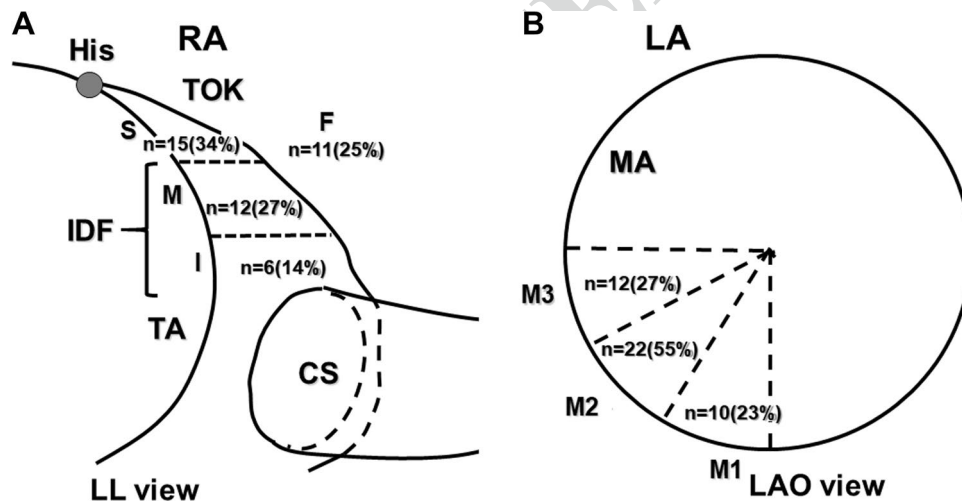


**Fig. 2** Schematic presentation of the triangle of Koch (TOK) of the right atrium (RA) in the left lateral (LL) view (A) and the mitral annulus (MA) of left atrium (LA) in the left anterior oblique view (B). A: TOK was divided into 3 parts (superior third part, middle third part, and inferior third part were defined as site S, site M, and

site I, respectively), and a part posterior to the TOK was defined as site F. B: MA was divided into 3 parts. The direction of 6–7, 7–8, and 8–9 o'clock of MA were defined as site M1, site M2, and site M3, respectively. His, His bundle electrogram recording site; TOK, triangle of Koch; IDF, inferiorly dislocated AFp

**2.5 Classification of the type of input site of the antegrade fast pathway by combining the right and left atria**

As shown in Fig. 3, by combining the AFpI[RA] (MinSt-V[RA]) and AFpI[LA] (MinSt-V[LA]) for the classification of the type of AFpI, the AFpI was classified into three

types: RA type, LA type, and bi-atrial (BA) type. The RA type was defined when the following two conditions were met: (1) the MinSt-V[RA] was shorter than that in the LA, and (2) there was no site on the shortest distance between the MinSt-V[RA] and MinSt-V[LA] along the atrial septum where the St-V interval was longer than the MinSt-V[LA]. In the RA type, the MinSt-V[RA] was the only AFpI

145  
146  
147

148  
149  
150

151  
152  
153  
154  
155  
156  
157

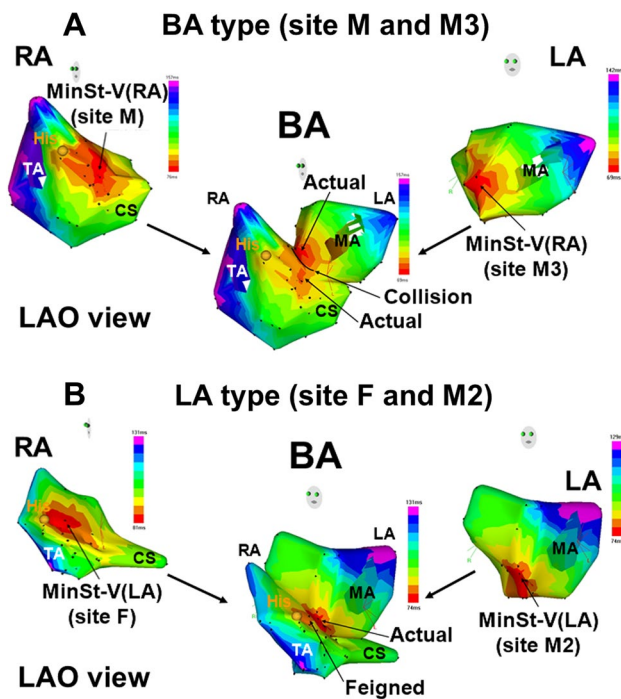


**Fig. 3** Examples of AFpI of BA type (A) and LA type (B) using 3-D bi-atrial St-V map. **A:** In BA type of AFp, minimal St-V interval in RA and LA showed almost the same value. MinSt-V(RA) and MinSt-V(LA) were clearly separated with some sites on the shortest distance between MinSt-V(RA) and MinSt-V(LA) along the atrial septum where St-V interval was longer than both minimal St-V intervals in RA and LA. In BA type, both MinSt-V(RA) and MinSt-V(LA) represent two different AFpI (actual). **B:** In LA type of AFp, minimal St-V interval in LA showed smaller value than that in RA and there was no site on the shortest distance between MinSt-V(RA) and MinSt-V(LA) along the atrial septum where the St-V interval was longer than minimal St-V interval in RA. In LA type, MinSt-V(LA) represents the only AFpI (actual) while MinSt-V(RA) does not represent an AFpI (feigned)

158 (actual) and the MinSt-V[LA] was not the AFpI (feigned).  
 159 An LA type was defined when the following two condi-  
 160 tions were met: (1) the MinSt-V[LA] was shorter than that  
 161 in the RA, and (2) there were no sites on the shortest dis-  
 162 tance between the MinSt-V[RA] and MinSt-V[LA] along  
 163 the atrial septum where the St-V interval was longer than  
 164 the MinSt-V[RA]. In the LA type, the MinSt-V[LA] was  
 165 the only AFpI (actual) and the MinSt-V[RA] was not the  
 166 AFpI (feigned). A BA type was defined when the following  
 167 two conditions were met: (1) the MinSt-V[RA] and MinSt-  
 168 V[LA] exhibited almost the same value, and (2) there were  
 169 some sites on the shortest distance between the MinSt-  
 170 V[RA] and MinSt-V[LA] along the atrial septum where  
 171 the St-V interval was longer than both the MinSt-V[RA]  
 172 and MinSt-V[LA]. In the BA type, the MinSt-V[RA] and  
 173 MinSt-V[LA] were two separate AFpIs (actual).

## 2.6 Statistical analysis

Data are expressed as the mean  $\pm$  SD. Differences between the means were compared using a one-way analysis of variance or the Kruskal–Wallis test. A Levene’s test was used to check for the equality of variance. The differences in the proportions were compared using the chi-square test. A  $P < 0.05$  was considered statistically significant. All statistical analyses were performed with the Statistical Package for the Social Sciences for Windows software (SPSS, version 27, Chicago, IL, USA).

## 3 Results

### 3.1 Clinical and electrophysiological characteristics of the study population

As shown in Table 1, 66% (29/44) of the patients in this study population continued antiarrhythmic drugs during the procedure. In patients with WPW syndrome, the antiarrhythmic drugs were discontinued preoperatively. Twenty-nine of 34 patients with AF continued on antiarrhythmic drugs. Class I drugs were used in 13 patients (cibenzoline 7, pilsicainide 5, and propafenone 1), class II (bisoprolol) in 7 patients, and class IV in 9 patients (verapamil 4 and bepridil 5). No class III drugs were used. The mean left atrial volume index (LAVI) was  $40 \pm 14$  mL/m<sup>2</sup>. The A-H interval during sinus rhythm was  $94 \pm 16$  ms. The number of mapping points was  $29 \pm 9$  points in the RA and  $25 \pm 10$  points in the LA. The minimal St-V interval was  $162 \pm 45$  ms in the RA and  $161 \pm 42$  ms in the LA.

### 3.2 Location of the input site of the antegrade fast pathway in the RA

As shown in Fig. 2 and Table 2, the MinSt-V[RA] was observed at site F in 11 patients (25%), site S in 15 (34%), site M in 12 (27%), and site I in 6 (14%). An IDF was observed in 41% of the patients. There were no significant differences among these four groups with regard to the age, gender, type of arrhythmia, LAVI, A-H interval during sinus rhythm, minimal St-V interval, and site of the MinSt-V[LA]. The minimal distance between the His bundle electrogram recording site and MinSt-V[RA] did not correlate with the A-H interval during sinus rhythm (Fig. 4).

### 3.3 Location of the input site of the antegrade fast pathway in the LA

As shown in Fig. 2 and Table 3, the MinSt-V[LA] was observed at site M1 in 10 (23%), site M2 in 22 (50%),



**AQ2** **Table 1** Clinical and electrophysiological characteristics of the study population

|  | <i>n</i> = 44     |
|--|-------------------|
| Age (years) (mean ± SD)                                | 64 ± 14           |
| Male/female ratio                                      | 31/13             |
| Type of arrhythmia                                     |                   |
| Paroxymal AF/persistent AF/WPW syndrome                | 18/16/10          |
| Continuation of antiarrhythmic drugs ( <i>n</i> (%))   | 29 (66)           |
| Vaughan Williams classification (I/II/III/IV)          | 13/7/0/9          |
| LAVI (ml/m <sup>2</sup> ) (mean ± SD)                  | 40 ± 14           |
| A-H interval during sinus rhythm (ms) (mean ± SD)      | 94 ± 16           |
| Number of mapping points (mean ± SD)                   |                   |
| RA/LA  | 29 ± 9/25 ± 10    |
| Minimal St-V interval (mean ± SD)                      |                   |
| RA/LA  | 162 ± 45/161 ± 42 |
| Classification of the AFp (RA type/LA type/BA type)    | 11/8/25           |
| Site of the minimal St-V interval in the RA (S/M/I/F)  | 15/12/6/11        |
| Site of the minimal St-V interval in the LA (M1/M2/M3) | 10/22/12          |

*SD*, standard deviation

**Table 2** Clinical and electrophysiological characteristics of the sites showing the minimal St-V interval in the RA

|  | Site F ( <i>n</i> =11) | Site S ( <i>n</i> =15) | Site M ( <i>n</i> =12) | Site I ( <i>n</i> =6) | <i>p</i> value |
|--|------------------------|------------------------|------------------------|-----------------------|----------------|
| Age (years) (mean ± SD)                                | 69 ± 7                 | 67 ± 9                 | 64 ± 14                | 49 ± 28               | 0.112          |
| Male/female ratio                                      | 8/3                    | 9/6                    | 9/3                    | 5/1                   | 0.703          |
| Type of arrhythmia                                     |                        |                        |                        |                       |                |
| Paroxysmal AF/persistent AF/WPW syndrome               | 3/6/2                  | 7/6/2                  | 6/4/2                  | 2/0/4                 | 0.117          |
| LAVI (ml/m <sup>2</sup> ) (mean ± SD)                  | 48 ± 17                | 39 ± 11                | 37 ± 15                | 28 ± 6                | 0.155          |
| A-H interval during sinus rhythm (ms) (mean ± SD)      | 89 ± 14                | 96 ± 22                | 95 ± 14                | 97 ± 13               | 0.651          |
| Minimal St-V interval (ms) (mean ± SD)                 |                        |                        |                        |                       |                |
| RA   | 161 ± 50               | 174 ± 30               | 162 ± 46               | 149 ± 65              | 0.387          |
| LA   | 155 ± 48               | 170 ± 27               | 170 ± 42               | 145 ± 60              | 0.313          |
| Site of the minimal St-V interval in the LA (M1/M2/M3) | 1/7/3                  | 4/7/4                  | 5/3/4                  | 0/5/1                 | 0.242          |

215 and site M3 in 12 (27%). There were no significant dif-  
 216 ferences among these three groups with regard to the age,  
 217 gender, type of arrhythmia, LAVI, A-H interval during  
 218 sinus rhythm, minimal St-V interval, and site of the MinSt-  
 219 V[RA]. Interestingly, only sites F and S were recognized  
 220 in the LA type. The minimal distance between the His  
 221 bundle electrogram recording sites and MinSt-V(LA) was  
 222 not correlated with the A-H interval during sinus rhythm  
 223 (Fig. 4).

### 224 3.4 Type of the input site of the antegrade fast 225 pathway by combining the right and left atria

226 As shown in Table 3, the AFpI was classified as an RA  
 227 type in 11 (25%), LA type in 8 (18%), and BA type in 25  
 228 (57%). There were no significant differences among these  
 229 three groups with regard to the age, gender, type of arrhyth-  
 230 mia, LAVI, A-H interval during sinus rhythm, minimal St-V

interval, site of the MinSt-V[RA], and site of the minimal  
 231 St-V interval in the LA. Examples of the AFpI in the BA  
 232 type and LA type are shown in Fig. 3. Figure 3A shows an  
 233 example of a BA type, and the MinSt-V[RA] was site M  
 234 and MinSt-V[LA] site M3. The MinSt-V[RA] and MinSt-  
 235 V[LA] were 76 ms and 69 ms, respectively. There were some  
 236 sites on the shortest distance between the MinSt-V[RA] and  
 237 MinSt-V[LA] along the septal wall where the St-V interval  
 238 was longer than both the MinSt-V[RA] and MinSt-V[LA],  
 239 and the 3-D bi-atrial St-V map exhibited two clearly sepa-  
 240 rate AFpIs. Figure 3B shows an example of an LA type,  
 241 and the MinSt-V[RA] was site F and MinSt-V[LA] site  
 242 M2. The MinSt-V[RA] and MinSt-V[LA] were 81 ms and  
 243 74 ms, respectively. There was no site on the shortest dis-  
 244 tance between the MinSt-V[RA] and MinSt-V[LA] along  
 245 the atrial wall where the St-V interval was longer than the  
 246 MinSt-V[RA], and the 3-D bi-atrial St-V map exhibited only  
 247 one AFpI.  
 248

**Fig. 4** Relationship between A-H interval during sinus rhythm and the minimal distance between His and AFpI (MinSt-V) in RA. There was no relationship between A-H interval during sinus rhythm and the minimal distance between His and AFpI (MinSt-V) in RA and LA.  $p=0.906$  (RA),  $p=0.606$  (LA)

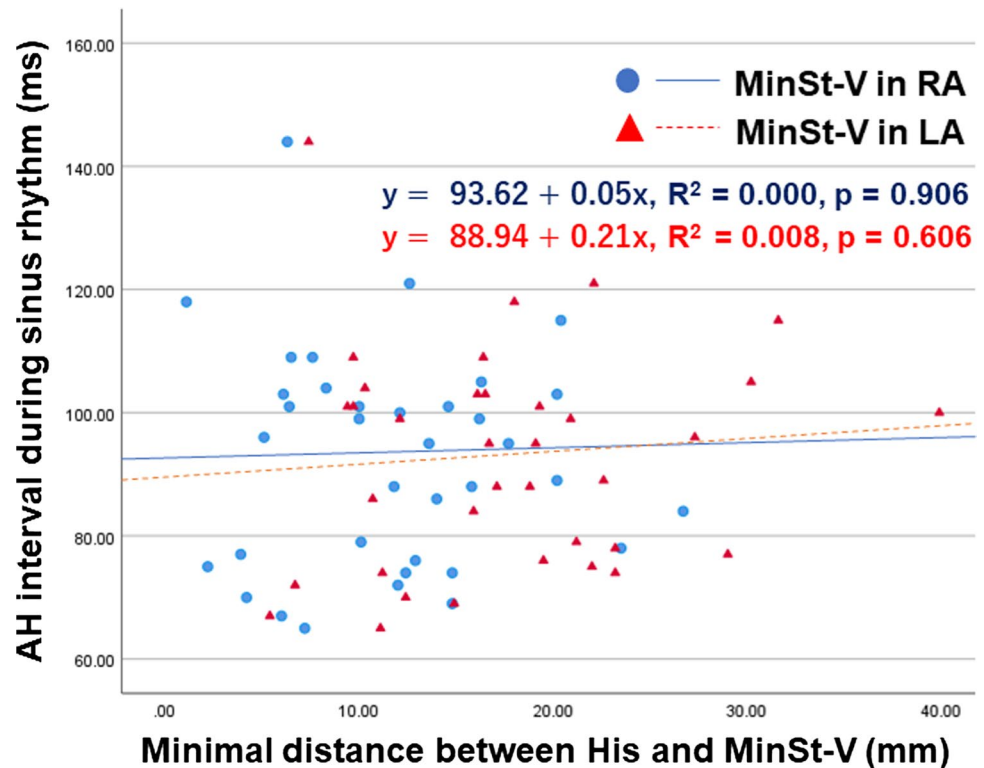


**Table 3** Clinical and electrophysiological characteristics of the sites with the minimal St-V interval in the LA

|   | Site M1 (n=10) | Site M2 (n=22) | Site M3 (n=12) | p value |
|---|----------------|----------------|----------------|---------|
| Age (years) (mean ± SD)                               | 66±10          | 68±12          | 56±17          | 0.06    |
| Male/female ratio                                     | 9/1            | 14/8           | 8/4            | 0.3     |
| Type of arrhythmia                                    |                |                |                |         |
| Paroxysmal AF/persistent AF/WPW syndrome              | 5/3/2          | 7/9/6          | 6/4/2          | 0.812   |
| LAVI (ml/m <sup>2</sup> ) (mean ± SD)                 | 31±11          | 45±16          | 38±12          | 0.08    |
| A-H interval during sinus rhythm (ms) (mean ± SD)     | 95±14          | 98±17          | 86±15          | 0.094   |
| Minimal St-V interval (ms) (mean ± SD)                |                |                |                |         |
| RA  | 170±42         | 161±51         | 157±40         | 0.547   |
| LA  | 166±40         | 160±50         | 161±31         | 0.784   |
| Site of the minimal St-V interval in the RA (F/S/M/I) | 1/4/5/0        | 7/7/3/5        | 3/4/4/1        | 0.242   |

## 249 4 Discussion

### 250 4.1 Major findings

251 In the present study, using the 3-D bi-atrial St-V map, it  
 252 was possible to classify the input sites of the AFp in both  
 253 the RA and LA. An AFpI[LA] was frequently observed and  
 254 was recognized in 75% of the patients. The AFpI[LA] and  
 255 AFpI[RA] were most frequently observed at site M2 (50%)  
 256 and site S (34%), respectively. The A-H interval during  
 257 sinus rhythm was not correlated with the minimal distance  
 258 between the His bundle electrogram recording sites and the  
 AK23 MinSt-V[RA] and MinSt-V[LA] (Table 4).

### 260 4.2 St-V map as an alternative to an St-H map

261 In the previous studies, the St-H map was the standard map  
 262 used for the determination of the AFpI [1–5]. In this study,  
 263 an St-V map was used instead of the St-H map because a  
 264 His catheter was not used in the majority of the patients  
 265 who had atrial fibrillation (77%) and the St-V map was  
 266 equivalent to the St-H map. As shown in Fig. 1, the St-V  
 267 interval (ai + b + c) was equal to the interval that consisted  
 268 of the St-H interval (ai + b) and interval between the onset  
 269 of the His bundle electrogram and peak of the QRS wave  
 270 in lead II (c). Here, the interval between the onset of the  
 271 His bundle electrogram and peak of the QRS wave in lead  
 272 II (c) was equivalent to the sum of the H-V interval and

**Table 4** Clinical and electrophysiological characteristics of the RA, LA, and BA type

|  |    | RA type (n=11) | LA type (n=8) | BA type (n=25) | p value |
|--|----|----------------|---------------|----------------|---------|
| Age (years) (mean ± SD)                                |    | 65±14          | 70±7          | 62±15          | 0.325   |
| Male/female ratio                                      |    | 10/1           | 4/4           | 17/8           | 0.143   |
| Type of arrhythmia                                     |    |                |               |                |         |
| Paroxysmal AF/persistent AF/WPW syndrome               |    | 4/3/4          | 4/3/1         | 10/10/5        | 0.751   |
| LAVI (ml/m <sup>2</sup> ) (mean ± SD)                  |    | 39±13          | 37±9          | 41±16          | 0.812   |
| A-H interval during sinus rhythm (ms) (mean ± SD)      |    | 97±20          | 104±12        | 90±15          | 0.094   |
| Minimal St-V interval (ms) (mean ± SD)                 | RA | 142±48         | 183±50        | 165±41         | 0.148   |
|  | LA | 157±45         | 159±46        | 163±42         | 0.899   |
| Site of the minimal St-V interval in the RA (F/S/M/I)  |    | 1/4/3/0        | 3/4/0/0       | 6/7/7/5        | 0.146   |
| Site of the minimal St-V interval in the LA (M1/M2/M3) |    | 3/5/3          | 2/6/0         | 5/11/9         | 0.366   |

273 ventricular activation time (VAT: the time from the onset  
274 of the QRS wave to the peak of the R wave). The H-V  
275 interval and VAT are reported to have a very high repro-  
276 ducibility with minimal variability [7–10]. Therefore, the  
277 St-V map was considered an alternative to the St-H map.

### 278 4.3 Left antegrade fast pathway input 279 to the atrioventricular node

280 To the best of our knowledge, this study was the first to  
281 investigate the detailed input site of the AFp in the LA.  
282 The 3-D bi-atrial St-V mapping with the CARTO system  
283 in this study revealed that an AFpI[LA] was present in  
284 75% of the patients and was the only AFpI in 18%. In the  
285 previous reports, an AFpI[LA] was suggested in cases with  
286 a left posteroseptal accessory pathway ablation [11, 12] or  
287 left-sided fast pathway ablation for typical atrioventricular  
288 nodal reentrant tachycardia (AVNRT) [13]. Moreover, the  
289 low success rate (46–69%) of a right-sided fast pathway  
290 ablation for AVNRT reported by Mitrani et al. may also  
291 suggest the residual presence of an intact AFpI[LA] after  
292 an AFpI[RA] ablation [14]. The only report about the  
293 probable presence of an AFpI[LA], by Gonzalez et al.,  
294 suggested that an AFpI[LA] existed with high probability  
295 in 95% of the patients [6]. That probability of the presence  
296 of an AFpI[LA] was higher than that in this study (75%),  
297 which was because atrial extrastimulation to identify the  
298 AFpI[LA] was used in their report.

### 299 4.4 Right antegrade fast pathway input 300 to the atrioventricular node

301 The 3-D bi-atrial St-V mapping with the CARTO system  
302 in this study revealed the presence of an AFpI[RA] in  
303 82% of the patients and only an AFpI in 25%. An inferiorly  
304 dislocated AFp (IDF) was recognized in 41% (18/44)

of the patients. The incidence of an IDF in this study was  
much higher than that reported by Delise et al. (10%) [2],  
but was similar to that reported in the other Japanese stud-  
ies (33–56%) [3, 4]. These differences might be related to  
the ethnic differences and therefore, further studies will be  
needed.

### 4.5 Clinical and electrophysiological indicators of the input site of the antegrade fast pathway

In this study, the clinical and electrophysiological indicators  
including the age, gender, type of arrhythmia, LAVI, A-H  
interval during sinus rhythm, minimal St-V interval, and site  
of the MinSt-V[RA] had no significant discriminating ability  
regarding the input sites of the AFp. Therefore, pending fur-  
ther studies, St-V or St-H mapping remains the only method  
for identifying the precise location of the AFpI.

### 4.6 Study limitations

- (1) This study was conducted at a single center and included only a small number of patients.
- (2) Antiarrhythmic drugs were continued in many patients (66%) because the majority of the patients studied had AF. Therefore, the St-V interval and other electrophysiological parameters could have been affected by those drugs.
- (3) Two different diseases, AF and WPW, were included in this study, and all AF patients were studied under deep sedation and all WPW patients under local anesthesia. Therefore, the difference in the disease and effect of the sedation could have affected the electrophysiological parameters. Further studies are needed to evaluate the effects of those.
- (4) In this study, we did not compare the effect of isoprenaline loading. The possibility that the input site of the

337 AFp could change according to the isoprenaline load-  
 338 ing remained.  
 339 (5) We fixed the pacing cycle length at 600 ms in order  
 340 to evaluate the AFp, to overdrive the sinus rate, and  
 341 to avoid Wenckebach periodicity. However, keeping a  
 342 uniform pacing rate might have led us to overlook other  
 343 concealed AV pathways.  
 344 (6) In this study, the St-V map was not compared with the  
 345 St-H map. Although further studies will be needed to  
 346 confirm this, it is reasonable to assume that the two  
 347 maps would be equivalent.

## 348 5 Conclusion

349 The 3-D bi-atrial St-V map could classify the input site of  
 350 the AFp in both the RA and LA. An AFpI[LA] was fre-  
 351 quently present and was recognized in 75% of the patients.  
 352 Except for the 3D bi-atrial St-V mapping, there were no sig-  
 353 nificant clinical or electrophysiological indicators that could  
 354 reveal the precise input site of the AFp.

355 **Acknowledgements** The authors thank Mr. John Martin for his linguis-  
 356 tic assistance with this manuscript.

## 357 Compliance with ethical standards

358 **Conflict of interest** The authors have no conflict of interest. This study  
 359 was approved by the institutional review board (IRB) of Tokushima  
 360 University, and the IRB approval number was 3851.

361 **Open Access** This article is licensed under a Creative Commons Attri-  
 362 bution 4.0 International License, which permits use, sharing, adapta-  
 363 tion, distribution and reproduction in any medium or format, as long  
 364 as you give appropriate credit to the original author(s) and the source,  
 365 provide a link to the Creative Commons licence, and indicate if changes  
 366 were made. The images or other third party material in this article are  
 367 included in the article's Creative Commons licence, unless indicated  
 368 otherwise in a credit line to the material. If material is not included in  
 369 the article's Creative Commons licence and your intended use is not  
 370 permitted by statutory regulation or exceeds the permitted use, you will  
 371 need to obtain permission directly from the copyright holder. To view a  
 372 copy of this licence, visit <http://creativecommons.org/licenses/by/4.0/>.

## 373 References

374 1. Delise P, Bonso A, Coro L, Fantinel M, Gasparini G, Themis-  
 375 toclakis S, Mantovan R. Pacemapping of the triangle of Koch: a  
 376 simple method to reduce the risk of atrioventricular block during  
 377 radiofrequency ablation of atrioventricular node reentrant tachy-  
 378 cardia. *Pacing Clin Electrophysiol.* 2001;24:1725–31.

2. Delise P, Sitta N, Bonso A, Coro L, Fantinel M, Mantovan R, Sciarra L, Zoppo F, Verlato R, Marras E, D'Este D. Pace mapping of Koch's triangle reduces risk of atrioventricular block during ablation of atrioventricular nodal reentrant tachycardia. *J Cardiovasc Electrophysiol.* 2005;16:30–5. 379  
 380  
 381  
 382  
 383  
 384  
 385  
 386  
 387  
 388  
 389  
 390  
 391  
 392  
 393  
 394  
 395  
 396  
 397  
 398  
 399  
 400  
 401  
 402  
 403  
 404  
 405  
 406  
 407  
 408  
 409  
 410  
 411  
 412  
 413  
 414  
 415  
 416  
 417  
 418  
 419  
 420  
 421  
 422  
 423  
 424  
 425  
 426  
 427  
 428  
 429  
 430  
 431  
 432  
 433

**Publisher's note** Springer Nature remains neutral with regard to jurisdictional claims in published maps and institutional affiliations.